



ORIGINAL ARTICLE

Co-cultured AuNP and Human Adipose MSCs could serve as a nano-drug system with tissue regenerative applications

Faezeh Salehi Nasab¹ , Mehdi Birjandi² , Bahram Rasoulian³ , Farzaneh Chehelcheraghi^{4*} ,
Marzieh Rashidipour^{5*} 

1. Student Research Committee, Lorestan University of Medical Sciences, Khorramabad, Iran.
2. Department of Nutritional Health Research Center, School of Health and Nutrition, Lorestan University of Medical Sciences, Khorramabad, Iran.
3. Department of Physiology and Pharmacology, School of Medicine, Lorestan University of Medical Sciences, Khorramabad, Iran.
4. Gastroenterology and Liver Diseases Research Center, Research Institute for Gastroenterology and Liver Diseases, Shahid Beheshti University of Medical Sciences, Tehran, Iran.
5. Nutritional Health Research Center, Lorestan University of Medical Sciences, Khorramabad, Iran.

ARTICLE INFO

Received: 2025/10/1
Revised: 2026/01/25
Accepted: 2026/02/14

*Corresponding:

Farzaneh Chehelcheraghi

Address:

Gastroenterology and Liver Diseases
Research Center, Research Institute
for Gastroenterology and Liver
Diseases, Shahid Beheshti University
of Medical Sciences, Tehran, Iran.

E-mail:

fr.Chehelcheraghi@gmail.com,
Chehelcheraghi.farzaneh@sbmu.ac.ir

*Co-corresponding:

Marzieh Rashidipour

Address:

Nutritional Health Research Center,
Lorestan University of Medical
Sciences, Khorramabad, Iran.

E-mail:

m_rashidi80@yahoo.com

ABSTRACT

Gold nanoparticles (AuNPs) are a suitable choice in the biomedical field due to their physical properties. The presence of gold nanoparticles, acting alongside mesenchymal stem cells (MSCs) through paracrine interactions, accelerates wound closure, enhances angiogenesis, favorably regulates extracellular matrix remodeling, and encourages skin regeneration with typical construction and function. In this study, we hypothesized that AuNPs Nano scaffolds would enhance the proliferation and specialization potential of human adipose-derived mesenchymal stem cells (hADSC in the wound area during *in vitro*, *In vivo* studies. To evaluate the nanoparticles; transmission electron microscopy was used to detect AuNPs and dynamic light scattering assay was used to estimate their size. Immunofluorescence staining, MTT assay, and semi-quantitative histological analysis were performed. Our results show that AuNPs at non-toxic concentrations (6 ppm) improve collagen content deposition and micro vessels expression induces cell migration and therapeutic efficacy in wound healing by hADSC at 14 and 28 days after surgery. As a result, AuNPs promote differentiation through a paracrine signaling pathway. Therefore, hADSC cultured with AuNPs can be used as a reagent to enhance skin tissue formation.

Keywords: Dynamic Light Scattering, Paracrine Communication, Metal Nanoparticles, Collagen, Fluorescent Transmission, Cell Proliferation, Angiogenesis

Cite this article: Salehi Nasab F, et al. Co-cultured AuNP and Human Adipose MSCs could serve as a nano-drug system with tissue regenerative applications. International Journal of Molecular and Cellular Medicine. 2026; 15 (1):1171-1182. DOI: 10.22088/IJMCM.BUMS.15.1.1171



© The Author(s).

Publisher: Babol University of Medical Sciences

This work is published as an open access article distributed under the terms of the Creative Commons Attribution 4.0 License (<http://creativecommons.org/licenses/by-nc/4>). Non-commercial uses of the work are permitted, provided the original work is properly cited.

Introduction

The utilization of nanoparticles can result in numerous applications, such as wound dressings, photodynamic therapy, delivery of therapeutic agents, sensors, probes, and diagnostics. Gold nanoparticles (AuNPs) are widely utilized in regenerative medicine research and have garnered significant interest in this field.(1, 2). Biological barriers can be crossed by nanoparticles, and their surface chemistry can be altered, which is linked to the enhanced safety of nanoparticles. In general, the reaction rate of nanoparticles exceeds that of macroparticles, with this property being dependent on factors such as a higher surface-to-volume ratio, chemical activity, and cellular uptake in nanoparticles. When nanoparticles interact with other compounds, biochemical reactions can lead to a reduction in cellular viability in their presence. The cytotoxicity of silver nanoparticles with a diameter of less than 20 nm surpasses that of larger nanoparticles.(3).

In the field of regenerative medicine, it is imperative to conduct thorough investigations into the toxicity of nanoparticles in order to ascertain their level of biocompatibility (4). Advanced therapeutic strategies utilize smart culture media to achieve biocompatibility of scaffolds capable of supporting transplanted cells. The smart culture media contains nanocomposites and nanomaterials, creating an environment similar to the body's natural tissue environment. In this environment, there is increased interaction with the cells of the damaged area, leading to accelerated regeneration (5). In the field of regenerative medicine, it is imperative to conduct thorough investigations into the toxicity of nanoparticles in order to ascertain their level of biocompatibility(6). Furthermore, it is anticipated that modern medicine will likely enhance the strength of scaffolds and improve the biological function of stem cells by utilizing the biomimetic properties of nanomaterials(7).

In modern treatments, the preferred action for burn wounds involves the use of human adipose-derived mesenchymal stem cells (hADSC). These cells are capable of secreting paracrine Vascular Endothelial Growth Factor (VEGF) and Fibroblast Growth Factor 2 (FGF-2). Significant immunomodulatory and proliferative capabilities are exhibited by these cells in comparison to other stem

cells (8). Stem cell transplantation is considered to hold great promise for the treatment of chronic diseases. However, its effectiveness is frequently hindered by challenges such as poor cell survival, incomplete differentiation, and insufficient cellular integration *in vivo*. To address these limitations, bio scaffolds that mimic the native tissue microenvironment have been developed by researchers. These scaffolds are designed to provide structural support and biochemical cues to guide cell behavior(9). Achieving this goal is currently not feasible due to several significant challenges. These challenges include burst drug release, insufficient cellular adhesion support, and a slow scaffold degradation rate (10).

Degenerative conditions and injuries result in an increasingly complex cellular environment, posing a significant challenge in the field of tissue engineering. Stem cell transplantation holds promise as a method for restoring tissue function, however, the inflammatory and inhibitory conditions in damaged tissues frequently hinder cell survival and integration. The extracellular matrix (ECM) of injured tissues commonly lacks the necessary supportive architecture for successful stem cell engraftment and differentiation (11-13).

The cellular response to scaffolds is to activate pathways via a combination of biological, biochemical, and biomaterial factors. Cells sense their surrounding environment and adjust their gene expression and functional behavior accordingly through mechanotransduction pathways.(14). Nanoparticles have the ability to alter the properties of culture scaffolds, including stiffness, surface charge, and topography, which in turn affects cell adhesion, proliferation, and lineage commitment (15, 16).

The physicochemical characteristics of the scaffold have been significantly modified by nanoparticles, which exhibit diverse sizes and shapes. Nanoparticles are particularly efficient in enhancing catalytic activity on surfaces, owing to their elevated surface-to-volume ratio, enhanced solubility, superior electrical and thermal conductivity, as well as improved catalytic performance.(17, 18). In the biomedical sector, AuNP can be applied across multiple areas.

Essential properties are required for effective drug delivery, cancer therapy, biomedical imaging, and diagnostic purposes. Additionally, there are unique

characteristics that set them apart from others, such as their remarkable compatibility with the human body, minimal toxicity, adjustable stability, small size, and capacity to engage with various substances (18, 19). The improvement of stem cell transplantation and the advancement of stem cell therapy could be achieved through the use of biodegradable gold nano scaffolds (19). Furthermore, the use of AuNPs in the culture medium resulted in highly reproducible outcomes, sustained multipotency, differentiation capabilities beyond passage 14, and therapeutic potential in Mesenchymal Stem Cells (MSCs) (20).

Unlike chemically synthesized AuNPs used in prior studies, our work utilizes laser-ablated, ligand-free AuNPs, providing a contamination-free nanosystem. This synthesis method produces highly pure nanoparticles without residual chemical stabilizers, allowing a clearer assessment of nanoparticle–cell interactions. Furthermore, our study uniquely examines long-term hADSC responses (up to 28 days) and identifies a reproducible, biologically safe concentration (6 ppm) for regenerative applications.

Considering the above points, this research aimed to provide a suitable solution for regenerative medicine by isolating and proliferating stem cells from human adipose tissue, while investigating the behavior of the cells in a gold nanoparticle nutrient culture medium and the possibility of their controlled proliferation. In this context, our study aimed to investigate the impact of different concentrations AuNPs on hADSC.

Methods

Preparation of Gold Nanoparticle (AuNP) Solution

The gold nanoparticle utilized in this study was prepared from a previous study, and its preparation is briefly outlined. The procedure involved performing laser ablation on a 99.99% pure gold disc. Prior to laser irradiation, the gold disc was immersed in a Branson high-frequency pressure (sound) waves cleaner for a duration of twenty minutes, followed by an additional cleaning after another 20 minutes. To avoid interactions with organic matter, the gold disc was rinsed with propanone. All AuNP preparations were filtered through 0.22- μ m filters and confirmed sterile and endotoxin-free.

For the synthesis of spherical gold nanoparticles, C12H25SO4Na was generated through the laser ablation of the gold disc in a dodecyl sulfate solution. In this research, the Quanta-Ray GCR170 Nd: YAG laser (wavelength 532 nm; pulse duration: 10 μ s; repetition rate: 10 Hz) was employed. After 22 minutes of photoablation, the color of the solution shifted to vermilion, signifying the formation of AuNPs. A 0.22 μ m filter was employed to filter the AuNP stock solution, which had a concentration of 100 ppm, from HISTOGENOTECH (LOT NO H990I, Tehran, Iran) (Description of materials in the supplementary file) (21).

Cell Culture, Proliferation

Human Adipose fatty tissue was used as a source for the mesenchymal stem cells (MSCs), which was previously identified in our research (Code no. 11347IBRC C, Iranian Biological Resources Center (IBRC), Iran). The MSC was incubated at 37°C with a 5% CO₂ atmosphere in an DMEM culture medium that included 10% fetal bovine serum (FBS) and 1% penicillin/streptomycin antibiotics (100 U/mL (22, 23).

Viability Assays

The AuNP solution was combined with a culture medium, which was determined to contain M1V1 + M2V2 (where M represents the concentration of the solution), V = the volume of solution) using the mass conservation equation: M1V1 = M2V2. The AuNP solution was prepared in different concentrations, including 1.5, 3, 6, and 9 ppm. Before adding AuNP solutions. Only the culture medium was used for treatment of the Control groups (0 ppm of AuNPs). MTT test, was done then reading the plate with an ELISA reader, and the average of the absorbance of the replicate wells for each dose was taken. Finally, the average absorbance of each dose was divided by the absorbance of the control and multiplied by 100 OD. The resulting numbers indicate the percentage of viability. Then, the viability of each concentration was plotted in the form of a graph and the results were interpreted and analyzed based on the graph. These differences were further amplified with time (23).

Investigation of Biological Functions

One of the criteria for evaluating the biological activity of cells is their morphology or cell

morphology scoring. The following scoring was used to assess cell morphology: Score 1 is assigned to cells lacking branching and having a confluency of less than 30%. Score 2 belongs to cells that have little cell proliferation, and their confluency is between 30 and 50%. Score 3 is assigned to cells that have cell branches and a confluency between 50 and 80%. Finally, score 4 is given to cells that have more than 2 branches and their confluency is greater than 80%. Mesenchymal stem cells were stained with the fluorescent red dye 1-Carbocyanine, 1-Dioctadecyl 1-conjugated to 3,3,3,3 Tetramethyllicocarboyanine Perchlorate (CM-Dil 1:100) and DM-5.5. Before transfection, cells were incubated with CM-Dil at 37°C for 15 min. After ensuring a cell density of 80%, cells were resuspended with trypsin, 0.25% EDTA, and serum containing minimal essential nutrients and FBS. (Serum-free medium/MEM preferred) The culture medium was phenol-free and contained 1:1 DMEM, 1% streptococcal penicillin, 2 mM L-glutamine, and 0.1 g/L sodium pyruvate.

5 μ l of 1 mM dye solution was added to 1 ml of cell suspension at a concentration of 1×10^6 cells/ml and incubated for 20 min in the dark at 37°C. The cell plate was observed after 5 min of centrifugation at room temperature. After repeated centrifugation 3 times, unstained cells were separated. After labeling the cells with PBS, the cells were resuspended in fresh culture medium and incubated for 7, 14, and 28 days. After the incubation periods, the expression of each treatment was visualized by confocal microscopy (TCS SP5 Confocal, Jena, Germany). The expression of DPI in the cells was analyzed using Image J 5.0 software, developed by the National Institutes of Health in Bethesda, MD, USA.

Animal Model

In our research, we prepared, 30 male Albino Wistar rats, old 2–3-month weighing 300–350 g for surgical procedures. The rats were housed in separate plastic enclosures and provided with a standard 12–12 h light-dark cycle, normal humidity, and access to a special diet and water ad libitum. Each rat was intraperitoneally injected with Ketamine -Xylazine (frequently used for anesthesia in rats) dosage of 100 mg/kg and 150 mg/kg. Prior to the surgical procedures, the back hair of the rats was shaved using a sterile blade. A 5cm incision was made on the back of each rat. All animal experiments were carried out

in compliance with the ARRIVE guidelines and the regulations set forth by the Animal Care and Use Committee of Lorestan University of Medical Sciences (IR.LUMS.REC.1402.066), in addition to the National Institutes of Health Guide for the Care and Use of Laboratory Animals.

Glass coverslips were coated with 6ppm of AuNP (1ml volume implanted surgery site) on both sides and implanted in 6-well culture plates for 30 minutes. The implanted AuNP cells were then treated after applying local anesthesia and making a 10 mm cut in the dorsal skin of the rats. After one week of subcutaneous implantation, the surrounding wound tissues containing the implanted AuNP cells were extracted for histological measurements. All the rats were euthanized with intraperitoneal injection of sodium pentobarbital (150 mg/kg, i.p.).

Tissue samples were extracted, fixed with 10% neutral buffered formalin, and embedded in paraffin seven days after implantation. The specimens were processed for multiple evaluations, including capsule formation assessment using hematoxylin and eosin (H&E) staining, as well as collagen deposition measurement using Masson's trichrome staining. The intensity of the LM was quantified using Image J 5.0 software after observation through a Nikon e100 microscope in Tokyo, Japan. (22).

Experimental design and controls

In vitro: Each treatment group included at least three independent biological replicates (cells from separate culture preparations) and three technical replicates per biological replicate. Treatment groups were: 0 ppm (culture medium only, negative control), vehicle control (equivalent concentration of SDS used during AuNP preparation without AuNPs), and AuNP treatments at 1.5, 3, 6, and 9 ppm. A positive control for cytotoxicity (0.1% Triton X-100) was included in pilot assays to validate the MTT procedure. Where relevant, an ionic gold control (Au^{3+} salt) was used to distinguish particle-specific effects from ionic species. Sample sizes, chosen based on common practice in similar preclinical studies, were $N = 3$ biological replicates with 3 technical replicates per group provide sufficient power to detect large effects typical for cytotoxicity assays.

In vivo: animals were randomized into the following groups: surgery only, Cell-only (hADSCs without AuNPs), AuNP-only (1ml), and AuNP (1ml)

+ hADSC (1×10^6). Group sizes are reported for each experiment ($n = 10$ per group); animals were allocated randomly and outcome assessments were performed blinded to group assignment. For in vivo histology and semi-quantitative analyses, $n \geq 5$ animals per group was employed to allow detection of tissue-level differences.

Statistical Analysis

After collecting the data, the central and dispersion indices were calculated specific test: The experimental data were represented as mean \pm standard deviation (SD) with sample size ($n=30$). The number of biological and technical replicates for each experiment was stated in the corresponding subsections. All histological quantifications and image-based assessments were performed by an investigator blinded to treatment groups. Animals and cell culture samples were randomized to treatment groups to minimize bias in allocation. One-way analysis of variance and LSD test were used to compare the mean differences between multiple

groups, and t-test was used to compare the mean differences between two groups. A $p < 0.05$ indicated that a difference was statistically significant.

Results

Characterization of AuNP

The preparation of AuNP solutions can be characterized by examining Figure 1A, which shows the brief procedure. Four groups were responsible for preparing the concentrations of AuNPs. 5, 3, 6 and 9 ppm. 0 ppm of AuNPs was found in the control group. Afterwards, different characterizations were applied to every AuNP solution prepared. The AuNPs in this research were observed using a transmission electron microscope, (Figure 1B). ImageJ software was used to quantify the AuNP diameter, which was determined to be 18.59 nm (Figure 1C). In Figure 1D, the particle size distribution is shown as a histogram, and the AuNP diameter was measured accurately at $45 < \mu\text{m} > 3.2$ nm (Figure 1E).

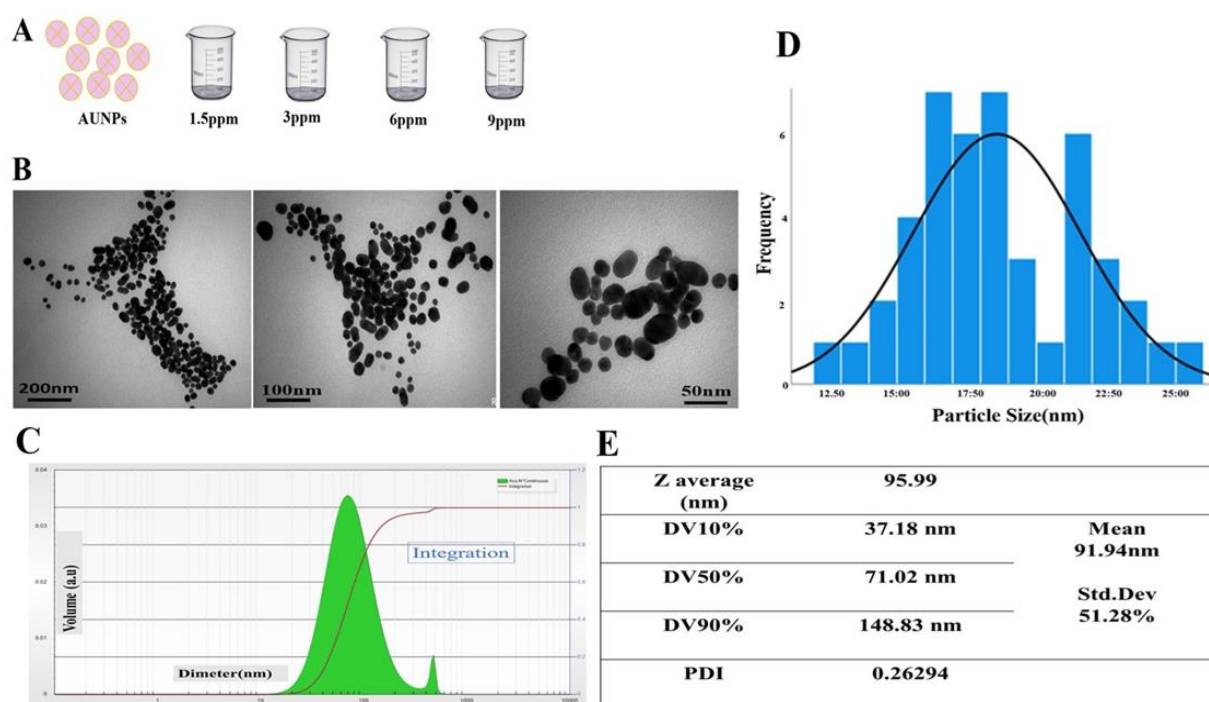


Figure 1. AuNP characterization. (A) Schematic of different AuNP concentrations of 1.5, 3, 6, and 9 ppm used in this study. (B) TEM(Transmission electron microscopy)of AuNP, from left to right. (C) The size of AuNPs (18.59 nm) was evaluated using ImageJ software. (D) DLS provided a measure of the hydrodynamic diameter of the AuNPs: Mean Number 1.93 nm, Mean Intensity 166.34 nm, Mean Volume 3.86 nm. (E) Table for Distribution statistics.

Cell viability, Safety and compatibility

Cell viability

The Safety and compatibility estimate of the AuNPs was accomplished. The cell viability percentage of the MSCs was activated pathway by the many AuNP treatments at 24h, 7, 14, and 28 days were explored and is proven in Figure 2A, with the formulation prearranged as Table S1 and Figure S1. At AuNP 1.25 and 2.5 ppm, the proliferation volume

of MSCs was significantly supported. Cell morphology; the MSCs' morphology characteristic was improved to be more extended while existence was preserved per 6 ppm AuNPs, suggesting, both cell adhesion and migration capacity were found to be significantly supported.

The overhead sign also illuminate, AuNPs at a concentration of 6 ppm are a better biocompatibility nanomaterial.

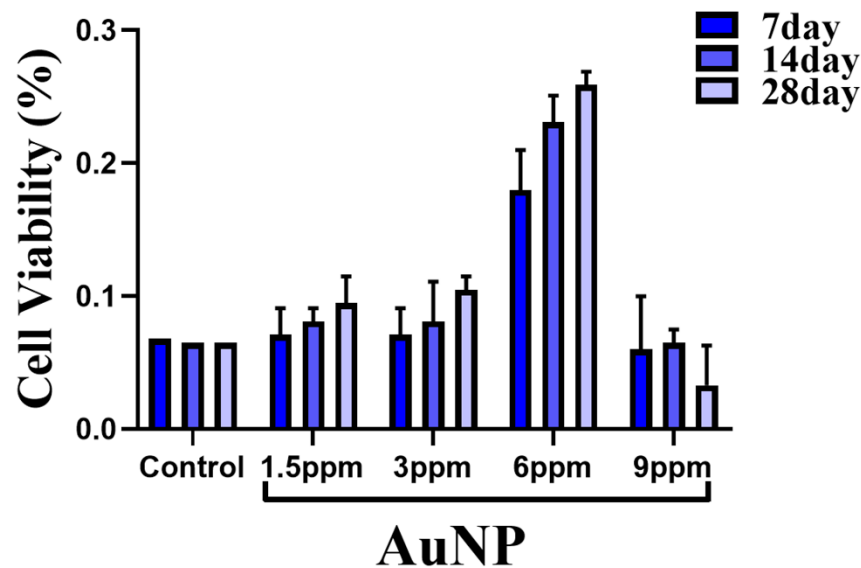


Figure 2. Cell viability of hADSC was preserved at many concentrations of AuNPs. (A) The cell viability of MSCs preserved with AuNPs was explored. The outcomes specify that the AuNP 6ppm treatment enhanced MSCs proliferation at 14 and 28, while the AuNP 9ppm treatments had significantly less cell viability at separate time points. The test results showed that on days 7, 14, and 28, there was no significant difference between the distribution of cell survival in the group exposed to gold nanoparticles (AuNP) (p value; 0.075, 0.06 and 0.148 where for day 7, day 14 and day 21 respectively) compared to the Control group.

To examine cell morphology and scoring, cells were first plated in 6-well plates and then exposed to gold nanoparticles (AuNP) and a control group. Cell morphology was examined on days 7, 14, and 28 after exposure. As shown in Figure 3A, on day 7, the control group scored 3, which meant more than 2 branches and a surface coverage of more than 70%. The group exposed to gold nanoparticles had similar morphology and scores. On day 14, the control group scored 1, which meant no cell branches and a surface coverage of less than 30%. In contrast, cells exposed to gold nanoparticles scored 4 because of their branches and surface coverage. On day 28, the score of the control group without exposure to gold nanoparticles decreased to 2, indicating the presence

of little cell proliferation, no branches, and 30–50% surface coverage. On the same day, cells exposed to gold nanoparticles received a score of 4 due to branches and the amount of surface coverage. Overall, exposure to gold nanoparticles increased cell growth on days 14 and 28 compared to the control group. MSCs were observed by confocal microscopy, the adjacent of light of AuNPs was analyzed using ImageJ, demonstrating the higher countenance in both 14 and 28 days, 6 ppm AuNP treatments. However, statistical analysis showed that there was no significant difference in the morphological distribution of cells between the two groups on these days. Morphological changes on days 14 and 28 are shown in Figure3 (Table S1-S4).

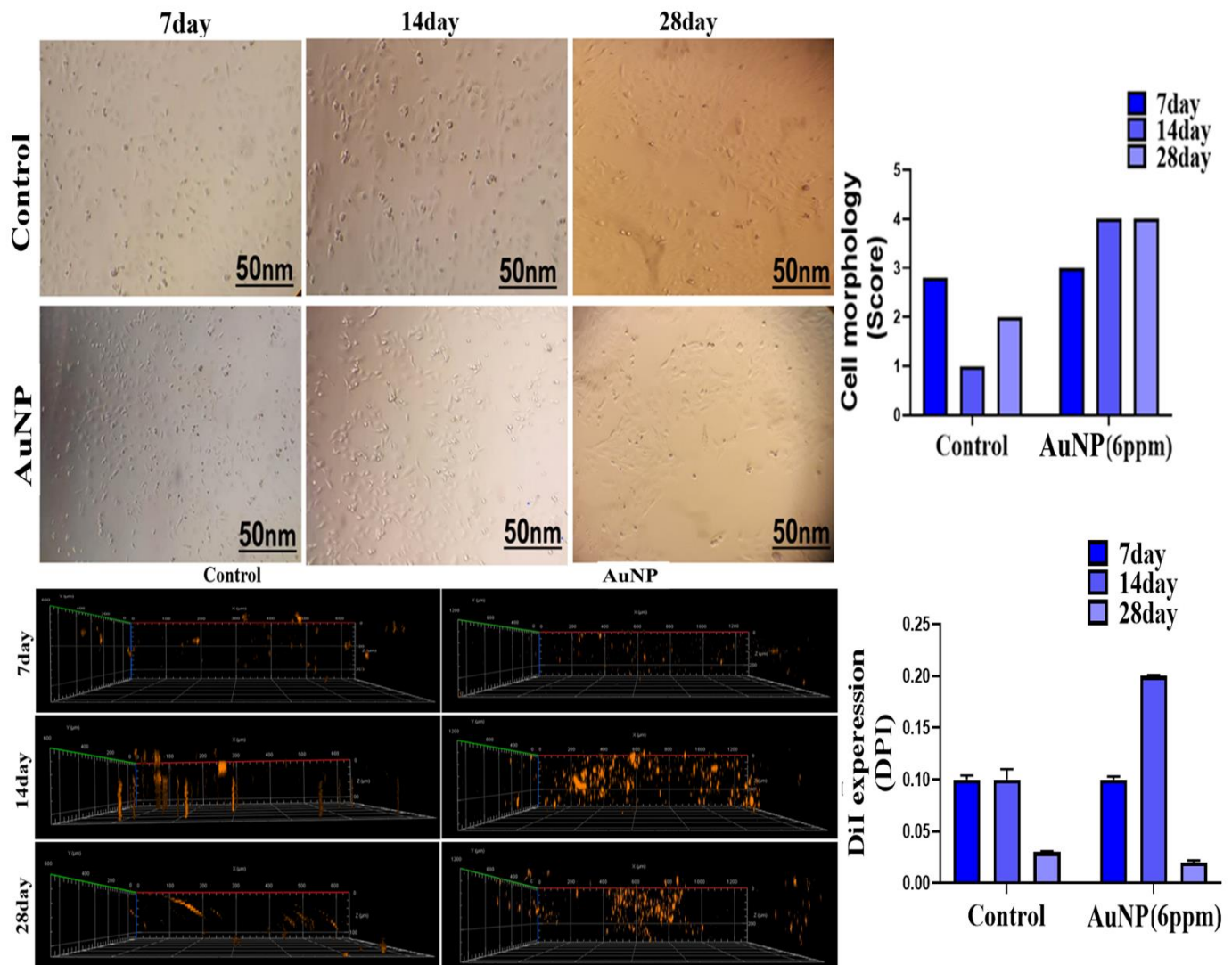


Figure 3. Biocompatibility of MSCs cells subsequently AuNP treatments. (A) MSCs morphology next 7, 14, and 28 days of AuNP (6 ppm) treatments was explored via LM. **(B)**The morphology characteristic scores of MSCs were quantified intended each day of handlings. The results elucidate that the 6 ppm AuNP group in 14 and 28 days had a higher MSCs amount score but no significant (p value 0.2,0.1 and 0.1 day7, day14 and day21 respectively). **(C)** A DiI expressed in MSCs is demonstrated using the IF staining method after days of handlings. By confocal microscope, DiI solution, orange-red-fluorescent dye fluorescence shows the countenance of hADSC. Scale bar = 100 μ m **(D)** MSCs higher countenance in 14 and 28 days, 6 ppm AuNP treatments (p value 0.05,0.03 and 0.03 day7, day14 and day21 respectively). The above consequences are represented as mean \pm SD. * $p < 0.05$, # $p > 0.05$.

Safety and compatibility *in vivo* study

Safety and compatibility calculations of nanomaterials with lasting inflammation have been an alarm for tissue renewal efficiency. Figures 4 demonstrate the serial histology examinations. The tissue images investigated in Figure 4A are shown using Masson's trichrome staining assay, and the blue color represents collagen deposition. After 6ppm AuNPs implantation, collagen deposition quantitative

results show a significant decrease, as depicted by Figure 4B. In Figure 4C, the formation of capsules was shown using histological images and H&E staining. Each treatment has white arrows that pinpoint the thickness of the capsule in the tissue. Figure 4D shows a trend similar to collagen deposition, which was partially quantified and shown. In the following step, LM images and semi-quantified data, as well as the expression of an endothelialization

marker, were evaluated. The research suggests that 6ppm AuNPs cause a significant increase in endothelialization in tissue, as shown in Figure 4.

During 28 days of AuNPs treatments, safety and compatibility investigations were performed in the rat model.

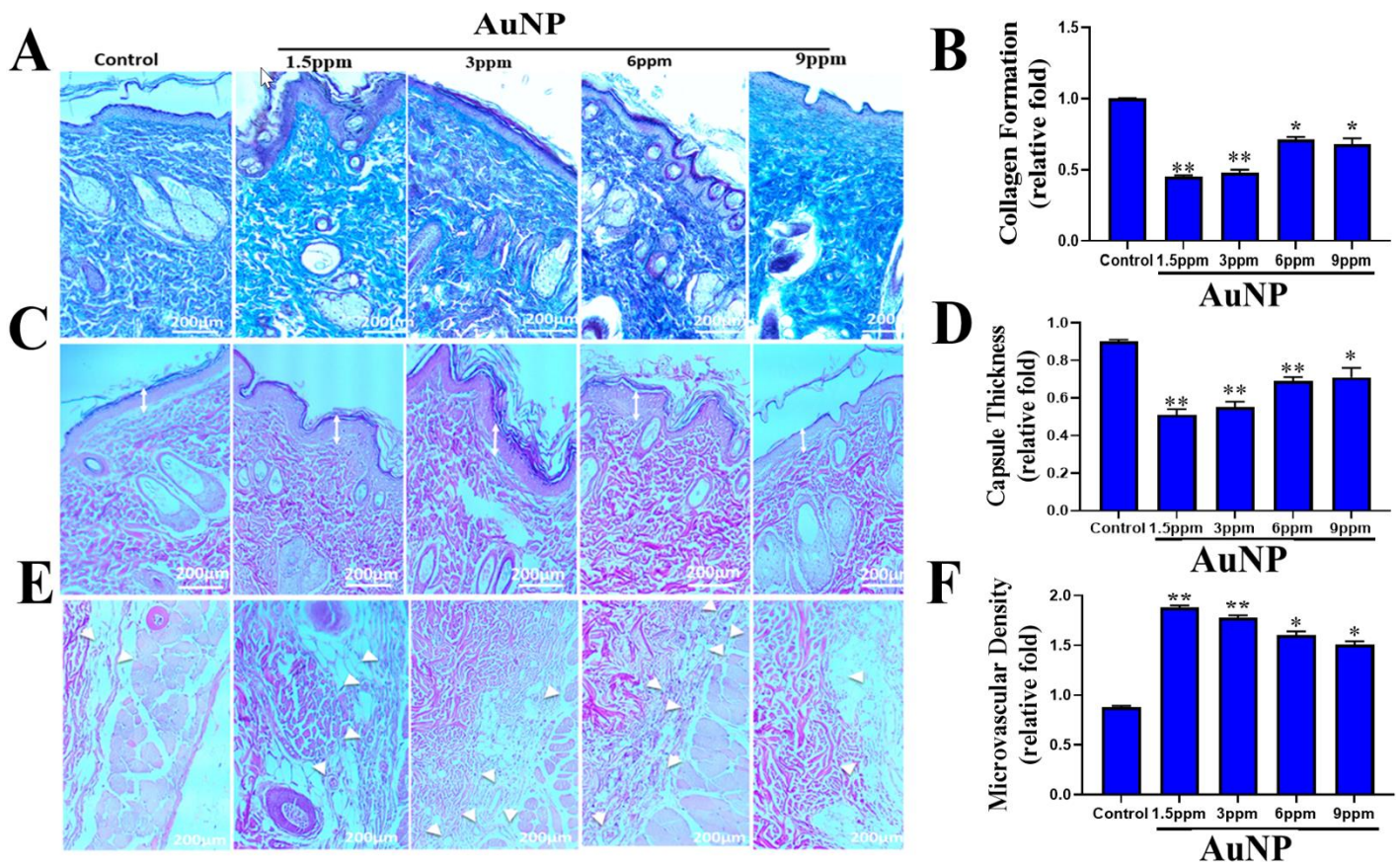


Figure 4. Masson's trichrome staining assay was employed to measure collagen deposition (blue color). By performing an H&E staining assay, the white double arrow shows the formation of the capsule. After histological staining, it was observed that the endothelial tube appeared. The formation of tubes was present below the skin. The scale bars of images were equal to 200 μ m. AuNP treatments had an impact on the semi-quantitative results of collagen deposition. A semi-quantitative measurement was done to determine the thickness of the tissue capsules in each treatment. Quantifying the intensity of endothelial tube formation was done too. Using AuNPs at 6 ppm could result in the most severe foreign body response and a significant boost in endothelialization for tissue regeneration, according to the evidence mentioned above. A, B: collagen formation, in control and concentrations of AuNP groups.

Collagen formation p value: 0.044, capsule thickness pvalue: 0.0001 and microvascular density pvalue:0.0001 C, D: capsule sickness, In control and concentrations of AuNP groups, E, F: micro vascular density, In control and concentrations of AUNP groups. Values are presented as the mean \pm SD (p < 0.05: *P, p < 0.01: **P, p < 0.001: ***P) and (n = 3).

Discussion

The constancy of gold nano particles (AuNPs) and their changeability make them an attractive choice for drug delivery with the addition of biological factors, AuNPs can be further steadied .Use of AuNPs for live tissue in human body applications has previously been described (18, 24). Nanotechnology has developed a

new approach to regenerative medicine by using metallic nanoparticles (MNPs). Various biocompatible NPs have been suggested in recent times to enhance wound healing. Previous literature has shown that collagen that has been modified with silver nanoparticles has the potential to differentiate MSC endothelial during vascular regeneration. Good

biological performance was observed in the combination of fibronectin and silver nanoparticles. Although AuNPs were incorporated into the culture system, we carefully evaluated their potential interference with hADSC behavior using multiple independent assays. First, a full dose–response viability analysis (1.5, 3, 6, and 9 ppm) was performed, and 6 ppm was identified as a non-toxic and non-inhibitory concentration, showing no significant reduction in hADSC viability compared with the control group at 7, 14, and 28 days (Figure 2; Tables S3–S4). Second, cell morphology scoring, proliferation behavior, and DiI-based expression analyses demonstrated that cells cultured with 6 ppm AuNPs maintained typical MSC characteristics and did not exhibit abnormal differentiation or stress-related morphology (Figure 3). Additionally, *in vivo* biocompatibility was confirmed by the absence of adverse foreign-body responses and normal collagen deposition patterns, indicating that AuNPs at the selected concentration did not negatively affect cellular or tissue-level pathways (Figure 4). Therefore, our data collectively support that 6 ppm AuNPs act as a biocompatible and non-interfering nanomaterial, and a separate control scaffold was not required beyond the pure culture medium (0 ppm) used as the negative control.

AuNPs and their nanocomposites for intra systemic uses. To use biomaterials in clinical settings, they must undergo thorough examination in regenerative medicine and tissue engineering. We aim to produce biomedical nanomaterials that are less immunogenic and offer better bio-efficient capacities (25). The transformation of young cells at early passages into immortalized cells is a challenge for standard h-ADSC culture protocols. Furthermore, the exclusion of senescent cells led to h-ADSC cultures with a large proportion of cells that were uniform in size, with 86% of them belonging to the restricted group. Using our strategy of removing cells that had an increase in granularity, size, or both in hADSC cultures reduced cell size variability in 3 out of 4 culture groups. By removing senescent cells, hADSC cultures showed increased cell consistency (86.8% within the expected gated population) and better purity. Additionally, the combinatorial approach of using AuNPs with concentration and size (6 ppm and 18.9 nm respectively) and increased time takes to generate a large number of h-ADSCs (p0 to

p1) from a traditional 5-6-weeks period until one to two weeks increased cell number and density, and minimized the presence of senescent cells (26).

The study examined the ratios of cell activation and proliferation conversion in 6 ppm AuNP treatments. According to the previous study, the survival of flaps in rats significantly increased by AuNPs and CEET treatment. Activation, proliferation, and survival of human ADSCs were induced by 6 ppm of AuNPs on days 14 and 28, as demonstrated by our results, suggesting that the immune system could handle treatments the concentration. Furthermore, the apoptosis ratio of AuNP was investigated. Our analysis shows that at a 6 ppm AuNPs concentration, MSCs exhibited a significantly lower apoptotic or molecular control point sensitivity compared to 9 ppm.

It was proven that the proliferation of hADSC was caused by the right amount of AuNPs. Gold nanoparticles can affect the regulation of apoptotic-related proteins, which is also a concern. Ant apoptotic proteins would be induced by the biocompatible nanomaterials. Days 14 and 28 saw better biocompatibility for further applications with AuNPs at concentrations of 6 ppm, as confirmed by the evidence. MSCs have been demonstrated as therapeutic agents in numerous environments, and a range of research suggests that they have therapeutic applications in cardiovascular disease pathologies. By enhancing our understanding of MSC biology, we may be able to refine MSC culture practices to enhance therapeutic applicability, which is an important point.

AuNPs by themselves lack antibacterial activity and, are combined with various bio macromolecules including chitosan, gelatin, dextran/polyvinyl alcohol, poly(lactic-co-glycolic acid)/poly(caprolactone), and cotton fabric to enhance the effectiveness of the wound healing process (27). Our histological finding showed interacting effect of AuNPs and hADSCs in Wound healing process (Fig 4 A, B). For example, collagen has been used as a cross-linking agent to help gold nanoparticles combine with other bio macromolecules including polysaccharides, peptides and growth factors, making them biocompatible and biodegradable for use as wound dressings. In addition, gold nanoparticles (AuNPs) have been conjugated to other nanoparticles, biomolecules, stem cells, and specific antibodies to enhance their antimicrobial

activity. The synergistic effect of gold nanoparticles with stem cells increased the paracrine properties of stem cells, which can be seen in the graphs of Figure 4 with changes in the rate of angiogenesis (Figure 4E and F) and increased epidermis thickness (Figure 4C and D). This synergy was also due to the size of the gold nanoparticles, which was less than 20 nm, which enhanced the paracrine effect of stem cells. In addition to biocompatibility, the toxicity level was also lowest at a concentration of 6 ppm (Figure 1E and D).

The use of metallic nanoparticles (MNPs) and macromolecules of interest such as Metal-organic frameworks (MOFs) is a novel approach to regenerative medicine that can be obtained through nanotechnology. A number of biocompatible NPs have been proposed for the improvement of wound healing (28). The use of MNPs like silver, gold, and zinc oxide has been shown to have beneficial qualities, including low *in vivo* *in biotoxicity* and bacteriostatic and bactericidal activity. The physicochemical properties of NPs are better due to their smaller mean size, increased surface area, and aspect ratio. Stimulating different cellular and molecular processes can alter the wound microenvironment's antibacterial, anti-inflammatory, and angiogenic activity, transforming it from a non-healing to a healing environment (24).

The free radical scavenging activity of AuNPs accelerates *in vitro* wound healing (29). Gold nanoparticles with chitosan bound demonstrated a substantial increase in free radical scavenging activity and improved biocompatibility compared to the pure nanoparticles(30).

Incorporating gold nanoparticles into co-cultured media-based and ADSCs wound treatments was a factor in the increase in hemostasis, epithelial tissue formation with a high healing rate, and rapid wound closure, which we found in our study. Moreover, utilizing hADSCs bound to AuNPs on the surface of incisional skin contributed to increased wound healing rates, reduced inflammation, and improved collagen deposition.

In addition, the results of *in vivo* experiments demonstrated that 6 ppm AuNPs decreased foreign body responses and had a superior retention efficacy with tissue integrity in an animal model. In closing, the evidence suggests that AuNP could be viewed as a promising system for delivering Nano drugs in a biosafety fashion in the process of developing

regenerative medicine with hADSCs mesenchymal stem cells.

The biomedical applications were promising because the physically synthesized AuNPs at the right concentration were a promising candidate. Biopolymers like collagen or polyethylene glycol can functionalize the particle surface, leading to its application as a safe-compatible nano-drug delivery structure with more permanency.

This research suggests that polymeric biomaterials-fabricated AuNPs with minimal toxicity effects without using reducing agents are more potential for clinical applications and have good biosafety. Also, AuNPs that can carry different biomolecules can be created to facilitate specific differentiation pathways in MSCs and improve tissue repair for investigations. Confocal microscopy findings confirm the biocompatibility and viability of stem cells co-cultured with AuNPs on day 28, which emphasizes the suitability of the gold nanoparticle fabrication method in this study (Figure3 C&D). It also shows that AuNP as Extra cellular matrix (ECM) regulate microvessels density through various signals, it is still unclear whether other pathways are involved. Further investigation of the mechanism of MSC proliferation with AuNP in promoting angiogenesis is necessary.

When co-cultured with AuNPs and MSCs, they can be utilized as a vehicle for delivering drugs to the site of inflammation or disease. In this study, it was demonstrated that 6 ppm AuNPs can promote proliferation and migration by activating molecular pathways. The stability of AuNPs was shown to suggest it could be a promising nanoparticle for future therapies. In general, the combination of gold nanoparticles and adipose-derived mesenchymal stem cells is an innovative drug delivery method with numerous advantages.

We believe that increasing the AuNPs concentration (6 ppm) can induce morphological changes during biomaterial modification, which can affect the binding potential of hADSCs. To enhance biocompatibility and organic targets in living tissues, such as attachment, proliferation, and anti-inflammation, it has been suggested that AuNPs at 6 ppm is the most effective concentration for biomaterial modification in hADSC culture media. The results of this study suggest that hADSC therapeutic strategies can be combined with AuNPs

physically synthesized at 6 ppm as a promising Nano platform for tissue regeneration. Recent research has shown that AuNPs incorporated into culture systems can help maintain the properties of MSCs, including pluripotency and viability over multiple passages.

Limitations

The identification of 6 ppm as a favorable concentration is based on viability, morphology, and tissue response rather than molecular signaling. Mechanistic events such as ROS modulation or activation of AKT/ERK pathways were not evaluated in the present study and will require future mechanistic work.

Funding

This research is taken from the thesis of general medicine student Faezeh Salehi Nasab, Grant (1397-1-99-2904)

References

- Giljohann DA, Seferos DS, Daniel WL, et al. Gold nanoparticles for biology and medicine. *Angew Chem Int Ed Engl.* 2010;49(19):3280-94
- Dykman L, Khlebtsov N. Gold nanoparticles in biomedical applications: recent advances and perspectives. *Chem Soc Rev.* 2012;41(6):2256-82.
- Katsumiti A, Gilliland D, Arostegui I, et al. Mechanisms of toxicity of Ag nanoparticles in comparison to bulk and ionic Ag on mussel hemocytes and gill cells. *PloS one.* 2015;10(6):e0129039.
- Yang M-Y, Liu B-S, Huang H-Y, et al. Engineered pullulan-collagen-gold nano composite improves mesenchymal stem cells neural differentiation and inflammatory regulation. *Cells.* 2021;10(12):3276.
- Jeong HJ, Koch A, Park S, et al. Bioactive scaffolds integrated with micro-precise spatiotemporal delivery and in vivo degradation tracking for complex tissue regeneration. *eong HJ, Koch A, Park S, et al. Bioactive scaffolds integrated with micro-precise spatiotemporal delivery and in vivo degradation tracking for complex tissue regeneration. Engineered Regeneration.* 2025;6:34-44. 2025;6:34-44.
- Bishop ES, Mostafa S, Pakvasa M, et al. 3-D bioprinting technologies in tissue engineering and regenerative medicine: Current and future trends. *Genes Dis.* 2017;4(4):185-95.
- Salyer CE, Bomholt C, Beckmann N, et al. Novel therapeutics for the treatment of burn infection. *Surg Infect (Larchmt).* 2021;22(1):113-20.
- Liu N, Zhou Z, Ning X, et al. Enhancing the paracrine effects of adipose stem cells using nanofiber-based meshes prepared by light-welding for accelerating wound healing. *Mater. Des.* 2023;225:111582.
- Chen F-M, Zhao Y-M, Jin Y, et al. Prospects for translational regenerative medicine. *Ethical Chall. Emerg. Med. Technol.* 2020:283-97.
- Esdaille CJ, Washington KS, Laurencin CT. Regenerative engineering: a review of recent advances and future directions. *Regen. Med.* 2021;16(5):495-512.
- Wang Z, Kapadia W, Li C, et al. Tissue-specific engineering: 3D bioprinting in regenerative medicine. *J. Control. Release.* 2021;329:237-56.
- Tabata Y. Significance of release technology in tissue engineering. *Drug Discov. Today.* 2005;10(23-24):1639-46.
- Das KK, Tiwari RM, Shankar O, et al. Tissue-engineered vascular grafts for cardiovascular disease management: current strategies, challenges, and future perspectives. *MedComm.* 2024;3(3):e88.
- Ding S-J, Yang D-J, Li J-L, et al. The nonmonotonous shift of quantum plasmon resonance and plasmon-enhanced photocatalytic activity of gold nanoparticles. *Nanoscale.* 2017;9(9):3188-95.
- Elahi N, Kamali M, Baghersad MH. Recent biomedical applications of gold nanoparticles: A review. *Talanta.* 2018;184:537-56.
- Ulfat I, Ahmed SA, Iqbal SMZ, et al. Synthesis and characterization of gold nanoparticles. *Adv. J. Sci. Eng.* 2020;1(2):48-51.
- Ahmed O, Sibuyi NRS, Fadaka AO, et al. Plant extract-synthesized silver nanoparticles for application in dental therapy. *Pharmaceutics.* 2022;14(2):380.
- Yu AY-H, Fu R-H, Hsu S-h, et al. Epidermal growth factor receptors siRNA-conjugated collagen modified gold nanoparticles for targeted

- imaging and therapy of lung cancer. *Mater. Today Adv.* 2021;12:100191.
19. Amgoth C, He Y, Wang S, et al. Metal (Au)-decorated chitosan-L-arginine polymeric vector for codelivery of gefitinib and miR125b for lung cancer therapy. *ACS Appl. Polym. Mater.* 2022;4(3):1675-87.
 20. Jia Y-P, Ma B-Y, Wei X-W, et al. The in vitro and in vivo toxicity of gold nanoparticles. *Chin. Chem. Lett.* 2017;28(4):691-702.
 21. Zhang Q, Hitchins VM, Schrand AM, et al. Uptake of gold nanoparticles in murine macrophage cells without cytotoxicity or production of pro-inflammatory mediators. *Nanotoxicology.* 2011;5(3):284-95.
 22. Hung H-S, Chang C-H, Chang C-J, et al. In vitro study of a novel nanogold-collagen composite to enhance the mesenchymal stem cell behavior for vascular regeneration. *PLoS One.* 2014;9(8):e104019.
 23. Lin R-H, Lee H-T, Yeh C-A, et al. Favorable biological performance regarding the interaction between gold nanoparticles and mesenchymal stem cells. *Int. J. Mol. Sci.* 2022;24(1):5.
 24. Sam S, Joseph B, Thomas S. Exploring the antimicrobial features of biomaterials for biomedical applications. *Results Eng.* 2023;17:100979.
 25. Hang Y, Wang A, Wu N. Plasmonic silver and gold nanoparticles: shape-and structure-modulated plasmonic functionality for point-of-care sensing, bio-imaging and medical therapy. *Chem Soci Rev.* 2024;53(6):2932-71.
 26. Boroujeni SN, Chehelcheraghi F, Khaksarian M, et al. Applying Vasopressin-Pre-Conditioned Human Adipose Mesenchymal Stem Cells Improves Heart Condition after Transplantation into Infarcted Myocardium *Int. J. Mol. Cell. Med.* 2022;11(3):207.
 27. Xia C, Ren B, Liu N, et al. A Feasible strategy of fabricating of gold-encapsulated dextran/polyvinyl alcohol nanoparticles for the treatment and care of wound healing. *J. Clust. Sci.* 2022;33(5):2179-87.
 28. Zeng Q, Qi X, Shi G, et al. Wound dressing: from nanomaterials to diagnostic dressings and healing evaluations. *ACS nano.* 2022;16(2):1708-33.
 29. Naraginti S, Kumari PL, Das RK, et al. Amelioration of excision wounds by topical application of green synthesized, formulated silver and gold nanoparticles in albino Wistar rats. *Mater. Sci. Eng. C.* 2016;62:293-300.
 30. Hsu S-h, Chang Y-B, Tsai C-L, et al. Characterization and biocompatibility of chitosan nanocomposites. *Colloids Surf. B.* 2011;85(2):198-206.